

1 **Chondrocyte protein co-synthesis network analysis links ECM mechanosensing to**
2 **metabolic adaptation in osteoarthritis**

3

4 Aspasia Destouni¹, Konstantinos C. Tsolis², Anastassios Economou², Ioanna

5 Papathanasiou^{1,3}, Charalambos Balis¹, Evanthia Mourmoura¹, Aspasia Tsezou^{1,3}

6

7 ¹ Laboratory of Cytogenetics and Molecular Genetics, Faculty of Medicine, University of
8 Thessaly, Larissa, Greece

9

10 ² KULeuven, Department of Microbiology, Immunology and Transplantation, Rega Institute
11 for Medical Research, Laboratory of Molecular Bacteriology, Leuven, Belgium

12

13 ³ Department of Biology, Faculty of Medicine, University of Thessaly, Larissa, Greece

14

15

16 **Corresponding author:** Professor Aspasia Tsezou
17 Laboratory of Cytogenetics and Molecular Genetics
18 Department of Biology, Faculty of Medicine

19 University of Thessaly

20 Biopolis, 41500

21 Larissa, Greece.

22 atsezou@med.uth.gr

23

24 **Keywords:**

25 Network co-synthesis analysis

26 Chondrocyte proteome

27 Osteoarthritis

28

29 **Running title:**

30 Osteoarthritis proteome network

31

32 **Abstract WORDS 168**

33 **Objective:** To systematically investigate the modular structure of the chondrocyte proteome
34 organisation in healthy and osteoarthritic (OA) cartilage.

35 **Design:** We implemented a systems approach by making use of the statistical network concepts
36 in Weighted Gene Co-expression Analysis to reconstruct the organisation of the core proteome
37 network in chondrocytes obtained from OA patients and healthy individuals. Protein modules
38 reflect groups of tightly co-ordinated changes in protein abundance across healthy and OA
39 chondrocytes.

40 **Results:** The unbiased systems analysis identified extracellular matrix (ECM) mechanosensing
41 and glycolysis as two modules that are most highly correlated with the disease. The ECM
42 module was enriched in the OA genetic risk factors tenascin-C (TNC) and collagen 11A1
43 (COL11A1), as well as in cartilage oligomeric matrix protein (COMP), a biomarker associated
44 with cartilage integrity. Mapping proteins that are unique to OA or healthy chondrocytes onto
45 the core interactome of ECM-mechanosensing-glycolysis identified differences in metabolic
46 and anti-inflammatory adaptation.

47 **Conclusion:** The interconnection between ECM remodeling and metabolism is indicative of
48 the dynamic chondrocyte states and their significance in osteoarthritis.

49

50

51

52

53

54

55 **Introduction**

56 Knee osteoarthritis (OA) is the second most common musculoskeletal disorder affecting
57 approximately 22.9% of individuals 40 years and over globally¹. The disease is phenotypically
58 heterogeneous with heterogeneity extending beyond histopathology to the predisposing risk
59 factors (reviewed in²). The lack of effective disease modifying drugs and preventive tools
60 highlights our incomplete understanding of the fundamental biological aspects of OA.

61 Large scale quantitative analyses of almost all molecular domains have aimed at elucidating
62 the molecular mechanisms underlying the cause and progression of osteoarthritis³⁻⁶.
63 Quantitative differences between the levels of gene transcription or proteins associated with
64 specific phenotypes represents only the first step of the systematic understanding of human
65 disease. In OA and healthy cartilage, the overlap between differentially expressed genes and
66 differentially abundant proteins is limited to 15-16%, likely owed to the alternative post-
67 transcriptional and post-translational control of protein levels^{4,5}.

68 It is known that most disease phenotypes are the end-product of the interaction between
69 proteins that mediate disease-associated processes. These biologically meaningful interactions
70 are well modelled by so-called “network modules” which in the case of proteomes represent
71 functionally coherent protein interactomes mediating the same biological processes⁷. Network
72 theory concepts have been used to study large-scale datasets obtained from a variety of
73 biological systems and have proven valuable for the dissection of biological mechanisms
74 contributing to complex diseases^{8,9}.

75 Our previous quantitative proteomic analysis revealed abundance differences between healthy
76 and OA chondrocytes in proteins enriched in metabolic and cytoskeletal processes, including
77 those of the tricarboxylic acid (TCA) cycle and adhesion, cytoskeletal remodeling and cell-
78 matrix interactions, suggesting a possible link between sensing of the ECM microenvironment
79 and regulation of metabolism through ECM-cell focal adhesion and cytoskeletal dynamics¹⁰.
80 Metabolic processes including lipid synthesis and glycolysis are regulated by changes in
81 cytoskeleton dynamics induced by sensing of the ECM mechanical properties (reviewed in¹¹).
82 Rewiring chondrocyte metabolism in the context of OA has been extensively studied¹² and
83 quantitative metabolomic profiling has revealed a link between chondrocyte metabolic
84 adaptation and physiological compressive mechanical loads¹³. However, how chondrocytes’
85 metabolism is regulated by the OA-altered ECM through mechanical cues caused by the
86 combination of ECM degradation and the increase in cell-cell adhesion in the proliferative
87 zone, remains elusive.

88 Here we revisited our previous proteomics dataset and implemented a systems modular
89 approach to reconstruct in an unbiased way the organisation of the chondrocyte proteome and
90 to parse the shared chondrocyte protein interactome in disease-associated modules.
91 Construction of the chondrocyte protein network yielded modules of tightly covarying proteins
92 which are associated with OA providing new insights into the connections between ECM
93 mechanosensing and adaptive changes in metabolism, anti-inflammatory and antioxidant
94 processes.

95

96 **Methods**

97 **Patients and proteomic data**

98 For the protein co-synthesis network analysis we used the common (shared OA-Normal)
99 processed spectral count data obtained from our published study (n=937), which are reported
100 in Suppl. Table 1¹⁰. Articular cartilage was obtained from 10 osteoarthritic patients who had
101 undergone total knee replacement surgery and 6 non-OA (termed healthy) adults. Peptides
102 were obtained by 1D-SDS-PAGE and in-gel digestion and were analyzed using nano-Reverse
103 Phase (RP) LC coupled to an LTQ-Orbitrap XL or an Orbitrap QE instrument. The Xcalibur
104 2.2 software (Thermo Scientific) was used for data acquisition. Protein abundance levels were
105 determined by counting label-free spectra by implementing the methods in the Scaffold
106 software, as previously described¹⁰.

107

108 **Data imputation and batch correction**

109 Missing peptide counts and variation owing to systematic biases are inherent problems of shot-
110 gun, label-free quantification¹⁴. We addressed these factors in our dataset by simulating the
111 dataset and imputing the missing values with Multivariate Imputation By Chained
112 Equations (MICE)¹⁵ and by correcting for batch effects with RUVseq¹⁶ package functions in
113 R. We implemented the MICE algorithm with 10 imputations using a predictive mean matching
114 model and a random number generator, seed=1 in log2 transformed data. To confirm the
115 reliability of the 1st imputation we tested the correlation between the imputed and raw data
116 (Pearson's $r=1$, $p<0.01$) (Fig.S1). We then upper-quantile normalized the simulated spectral
117 counts and corrected unwanted variation i.e. not explained by the experimental design by
118 implementing the RUVr function by factor analysis on deviance residuals after a running a
119 regression of the counts on the covariate of interest (disease status). We chose to exclude an

120 outlier healthy sample (X152) following unsupervised hierarchical clustering because it
121 mapped in the OA cluster (data not shown).

122

123 **Weighted gene co-expression analysis (WGCNA)**

124 WGCNA was performed with the tools in the WGCNA R package¹⁷ on the simulated and batch
125 corrected proteome data. We constructed a signed network of weighted correlations by
126 calculating a pairwise correlation matrix and then raising the co-expression measure to a power
127 $\beta=30$ to obtain the adjacency matrix. The power is a soft-threshold of the correlation matrix
128 and its value is set to preserve the scale-free topology of the network (Fig S1). To identify
129 “modules of co-synthesized proteins” in chondrocytes (hereafter “modules”) we calculated the
130 connection strength of each protein with all other proteins in the dataset and clustered the
131 proteins based on their topological overlap. Briefly, the topological overlap matrix (TOM) was
132 calculated (the strength of the correlation of 2 proteins with respect to all other proteins in the
133 network) and the TOM dissimilarity measure (1-TOM) was used in hierarchical clustering with
134 Ward’s minimum variance method. We used the Dynamic Hybrid Tree Cut algorithm to cut
135 the branches of the hierarchical clustering tree. Each branch represents a module, i.e. a group
136 of highly correlated protein levels across healthy and OA samples. We set the minimum
137 module size to 15 proteins. The expression profile of each module was then summarized by
138 calculating the first principal component termed as module eigenprotein (MEP) with singular
139 value decomposition of the scaled protein abundance. Modules whose MEs were highly
140 correlated ($r>0.8$) were merged into one module. Meta-modules are defined as modules that
141 form a single cluster in hierarchical clustering with the distance measure defined as 1-
142 corrMEPs. The power of trait-module correlations tests was adjusted for multiple testing with
143 the Benjamini-Hochberg method using R’s base function. Disease significance is the averaged
144 absolute correlation (r) between the MEP levels in a particular module with OA. Unsupervised
145 hierarchical clustering was performed with Euclidean distances using Ward’s minimum
146 variance method.

147

148 **Module annotation**

149 Over-representation analysis was run for the pathways, biological processes ontology domains
150 using the NIH NCATS Bioplanet 2019 database¹⁸ and other functional (GO Biological Process)
151 and disease databases (GWAS catalog 2019) in Enrichr¹⁹. Briefly, we mapped Uniprot IDs to
152 gene symbols and we submitted the protein list to the Enrichr web service. Of the 10 top terms

153 we determined the most relevant by considering the redundancy of the enrichment and those
154 with FDR<0.05.

155

156 **Network and data visualization**

157 Network visualization was performed in Cytoscape v.3.8.2. Known and predicted protein-
158 protein interactions (PPIs) with combined score of high confidence (>0.7) were obtained from
159 the STRING database²⁰. We parsed the PPI network by implementing an edge-weighted spring
160 embedded layout algorithm weighted by the String score into clusters of nodes that are highly
161 attracted and at the same time repelled from other nodes or clusters of nodes. Briefly, the
162 combined String score is computed by combining the probabilities from the different evidence
163 sources, correcting for the probability of randomly observing an interaction. Data visualization
164 was performed in R by using package built-in plotting functions and ggplot2²¹.

165

166

167

168

169 **Results**

170 **Chondrocyte protein co-synthesis network construction in osteoarthritic and healthy** 171 **cartilage**

172 We have previously identified 937 proteins shared between OA and healthy cartilage
173 proteome¹⁰. We now tested whether the shared chondrocyte proteome could be a classifier for
174 osteoarthritic and healthy cartilage. We found that two proteome clusters classify samples by
175 disease status and K/L score only and we therefore did not adjust for BMI, age or sex ~~K/L score~~
176 in subsequent analyses. Therefore, the shared proteome mediates biological processes that are
177 altered in chondrocytes damaged by OA compared to healthy cells.

178 We then implemented WGCNA and parsed the shared proteome in 13 groups of strongly co-
179 synthesized proteins termed modules (Fig. 1A, Fig. S1 and Table SII). Protein modules
180 commonly include the functional protein components of a specific biological process or
181 pathway²². We therefore tested which processes are represented by the module proteins and
182 found that the 13 modules differ in the top enriched functional terms (Table SIII). Specifically,
183 4 out of the 13 modules were associated with metabolic processes including glycolysis
184 (MEyellow), mitochondrial β -oxidation of unsaturated fatty acids (MEcyan), benzo(a)pyrene
185 metabolism (MEtan) and amino acid metabolism (MEblue) (Table SIII). Metabolic changes in
186 processes including fatty acid synthesis, amino acid synthesis, mitochondrial respiration and
187 glycolysis in chondrocytes have been associated with impaired chondrocyte function and

188 disease progression¹². MEGreenYellow is highly enriched in ECM-receptor interactions and
189 includes proteins with high biological relevance to articular cartilage integrity and OA biology
190 as COMP, COL11A1, COL6A2, TNC, fibronectin type I (Fn1) and hyaluronan and
191 proteoglycan link protein 1 (HAPLN1). MEbrown is associated with clathrin-derived vesicle
192 budding, a process that mediates exosome formation, which plays a role in articular cartilage
193 integrity maintenance (reviewed in²³). The pathway downstream of ERBB1- epidermal growth
194 receptor (EGFR) signaling (MEblack) is essential for the maintenance of chondrocyte growth
195 in the superficial zone of the articular cartilage²⁴. The top term for MEGreen is the mu-calpain
196 pathway and includes Rho GTPases RHOA, RAC1 and talin 1(TLN1).
197 Thus, WGCNA parsed the shared chondrocyte proteome in modules with biologically
198 meaningful enrichment in osteoarthritis associated processes.

199

200 **Chondrocyte proteome modules associate with osteoarthritis**

201 We hypothesized that the processes involved in impaired chondrocyte function and OA
202 pathology would be organized in modules that would be strongly associated with the disease.
203 To test this, we correlated the module protein synthesis levels to all traits (Fig. 1A) and found
204 that 5 of the 13 modules were strongly and significantly correlated with OA (Benjamini-
205 Hochberg, FDR<0.05) (Fig. 1A). To better understand the relationship between OA and the
206 module protein synthesis levels, we calculated the module Disease Significance (DS) (see
207 Methods) and found that MEblue, MEyellow, MEGreenyellow and MEGreen protein level
208 changes are associated with OA (DS>0.5)(Fig. 1B). Furthermore, MEblue, MEyellow and
209 MEGreenyellow form a meta-module (single branch in dendrogram, Fig.1A) representing the
210 higher-order organization of the proteins in these 3 modules.

211 We then hypothesized that the most essential proteins for the maintenance of healthy cartilage
212 would have tightly coordinated synthesis levels across samples and high disease significance.
213 In the chondrocyte network these parameters are represented by high intra-modular
214 connectivity and high DS (Fig. S3B,C). Our rationale is supported by evidence showing that
215 proteins with high module interconnections are commonly essential to the processes they
216 mediate²⁵ and are associated with disease²⁶. The meta-module comprises protein components
217 of ECM organization, integrin mediated focal adhesion, amino-acid and protein turnover as
218 well as glycolysis and general metabolism (Fig. 1C). Therefore, essential proteins involved in
219 glycolysis-gluconeogenesis are highly connected to key structural components of cartilage
220 ECM organization and focal adhesion in the meta-module (Fig.1C,D). MEGreen comprises
221 proteins involved in cytoskeleton dynamic changes in response to mechanical or ECM

222 remodeling stimuli, like the GTPase RAC1, the major cell surface adhesion molecule for
223 hyaluronan CD44, as well as proteins involved in translation and osteoblast differentiation
224 (integrin- α - β 3-osteopontin and sphingosine-1-phosphate S1P²⁷) (Fig. 1C ,Tables SIII and
225 SIV).

226 Meta-module protein levels display a strong negative correlation with OA highlighting the role
227 of ECM integrity and metabolism in chondrocyte-cartilage homeostasis. As expected from the
228 direction of the module-trait correlations, the abundance of the proteins in the meta-module
229 was increased in healthy compared to OA chondrocytes (Fig.1D). On the other hand, protein
230 levels in MEgreen are positively associated with OA and decrease in healthy compared to OA
231 cells (Fig.1D).

232 Altogether, this analysis suggests that highly coordinated protein abundance changes in
233 metabolic and ECM sensing processes are associated with healthy and OA chondrocytes.

234

235 **Overlap of the altered interactome with an independent OA chondrogenesis proteome**

236 We next sought to assess the degree of relevance between the chondrocyte proteome synthesis
237 changes and the reported protein changes during chondrogenesis. We obtained the overlaps
238 between our entire proteome (n=937) and the list of significantly up/down regulated proteins
239 (n=43) reported in Rocha et al.²⁸. Of the 43 significantly altered proteins, 37 overlapped with
240 the chondrocyte proteome (86.04%) and of those, 20 are members of the OA-associated
241 modules with the majority (12/20) mapping to MEyellow (Fig. S3). The direction of abundance
242 level changes is concordant for 16 of the 20 overlapping proteins. The concordant group
243 includes structural and matricellular cartilage ECM components (e.g. COL6A2, TNC), several
244 glycolytic enzymes (e.g. GAPDH, TP1, LDHA) and cytoskeleton structural proteins (e.g.
245 TPM4 and TLN1) (Fig.S3). Importantly, the proteins with discrepant changes are not essential
246 members of the chondrocyte modules.

247 From this comparison we conclude that the 16 concordant overlapping proteins are central to
248 the chondrocyte specific metabolic and cytoskeleton -ECM functions and that both glycolytic
249 enzymes and ECM components are depleted in OA compared to healthy chondrocytes.

250

251 **The chondrocyte protein interaction network links extracellular matrix remodeling to** 252 **glucose metabolism**

253 To assess the biological functional interactions between proteins in the meta-module and their
254 functional inverse relationship to the proteins in the MEgreen module. (Fig.2A) we next tested
255 the network for enrichment in protein- protein interactions in the STING database (PPI

256 enrichment , $p < e-16$). The parsed network yielded 3 prominent peripheral clusters with
257 functional distinctions including cartilage-ECM-focal adhesion, glycolysis-TCA cycle, protein
258 and amino-acid biosynthesis. The majority of essential proteins of the MEgreen module
259 (abundant in OA chondrocytes) are located at the center of the network (18/30 proteins)
260 including central components of integrin-focal adhesion (TLN1, RAC1, RHOA), cytoskeletal
261 dynamics (DSTN, CCT2, CCT8, TUBA1B) and protein turnover (PSMD, EIF, RPL). We
262 found that the top 20 proteins with the highest degree in the interactome, are important
263 glycolytic enzymes including GAPDH, TPI1, ALDOA, PGM1, GPI, ENO1, PGK1, LDHA,
264 PKM, LDHB, MDH1 (Fig. 2B). Top degree nodes include FN1, master actin tubulin folding
265 chaperones CCT2 and CCT8 of the CCT/TriC complex, P4HB a multifunctional enzyme
266 involved in the hydroxylation of the propyl residues in pro-collagen, the molecular motor
267 DYNC1H1 and chaperones HSP90B1 and HSPA8.

268 Mapping the PPI network onto module-eigen proteins corroborated the existence of functional
269 links between the processes of a core chondrocyte interactome which mediate the crosstalk
270 between ECM integrity -mechanosensing with glycolysis through the cytoskeleton.

271

272 **The unique interactomes of OA and healthy chondrocytes reveal differences in protective** 273 **and adaptive processes**

274 We next focused on the proteins which are unique to each condition (Tsolis et al.
275 Supplementary Table 1¹⁰), we mapped them on the shared network and created a healthy (n=11
276 unique proteins) and an OA (n=131 unique proteins) PPI network (STRING score>0.7). Our
277 rationale for the dichotomous mapping was that the protein level abundance changes in the
278 shared proteome might reflect the deregulation of a core chondrocyte homeostatic ECM
279 mechanosensing-metabolism interactome connected to unique OA or healthy proteins
280 mediating processes that are specific to either cartilage damage or maintenance.

281 Integration of the unique proteins from healthy controls didn't affect significantly the structure
282 or the topology of the core network because only four (SERPINA1, APOE, C3 and CRP) of
283 the 11 proteins yielded highly confident interactions (Fig. 3A). GAPDH remains the node with
284 the highest degree and Complement C3 is added in the top 20 nodes (Fig. 3B). Proteins with
285 protective (SERPIN1A and APOE) or enhancing (C3, CRP) functions in inflammation interact
286 with the core proteome. ApoE was recently shown to inhibit the Classical Complement
287 Cascade in atherosclerosis and Alzheimer's disease by forming a complex with C1q which is
288 activated in response to multiple stimuli such as oxidized lipids and oxidized-LDL²⁹.
289 SERPINA1 is an acute phase serine protease shown to be upregulated during chondrogenesis

290 from MSCs³⁰ and in response to IL-6 treatment of chondrocytes *in vitro*³¹. The integration of
291 these proteins in the core homeostatic interactome suggests that APOE and SERPINA1
292 probably act as check points to the burden of low-grade chronic inflammation (CRP, C3) on
293 cartilage integrity.

294 The network of proteins that are unique to OA comprises a total of 303 nodes expanding the
295 core interactome by 129 proteins. Chaperonin CCT2 is the top node followed by beta-catenin
296 (CTNNB1) (Fig. 4B). Two ribosomal proteins, Ribosomal Protein S4 X-Linked (RPS4X) and
297 Ribosomal Protein Lateral Stalk Subunit P0 (RPLP0) were added to the top node list because
298 their immediate interactors are uniquely identified in OA chondrocytes and comprise
299 translation initiation and elongation factors and ribosomal subunits. Elevated levels of β -
300 catenin are associated with cartilage degeneration and increased WNT signaling in mature
301 chondrocytes and exacerbate hallmarks of the manifestation of OA such as chondrocyte
302 hypertrophy and increased matrix metalloproteinase expression^{32,33}. In the OA interactome
303 CTNNB1 is linked to MMP14, which is secreted by invading osteoblasts in the cartilage
304 hypertrophic zone. This interaction probably indicates that MMP14 signals to promote
305 cartilage canal formation and secondary ossification center initiation³⁴.

306 Integration of phospholipid hydroperoxide glutathione peroxidase 4 (GPX4) connected the
307 proteins involved in glutathione metabolism (GSTM2, GSTM3 and GSS) to the core
308 interactome, which remained unconnected in the healthy network (Fig. 3A, Fig. 4A). GPX4 is
309 a key enzyme that reduces phospholipid hydroperoxides to alcohols and protects cells from
310 ferroptosis³⁵, a process of cell death. A cell density induced adaptive mechanism rescues cells
311 from the lipotoxic conditions by sequestering poly-unsaturated fatty acid (PUFA) TGAs in
312 lipid droplets (LDs) protecting cells from ferroptosis³⁶. Lysophosphatidylcholine
313 acyltransferase 1 LPCAT1, one of the Lands cycle key enzymes, responsible for phospholipid
314 remodeling at membranes, is exclusive to the OA interactome. LPCAT1 was found to localize
315 to the phosphatidylcholine (PC) monolayer membrane of the neutral triacylglycerol (TGA)
316 containing lipid droplet (LD)³⁷.

317 Mapping the OA and healthy PPI networks revealed differences in protective and adaptive
318 mechanisms in cartilage homeostasis.

319

320 **Discussion**

321 Cell functions are maintained by the coordinated activity of functional modules driven in part
322 by relatively synchronized protein abundance. Here we revisited our previous proteomics

323 dataset and implemented a systems approach using network concepts in Weighted Gene Co-
324 expression Analysis to reconstruct the organisation of the chondrocyte proteome.
325 We demonstrate that the shared synchronously changing proteome is parsed into functional
326 modules with well characterized significance to OA. As such, core structural components of
327 the cartilage ECM are abundant in healthy chondrocytes but depleted in OA, reflecting the
328 degradation and impaired homeostasis of the articular ECM.

329

330 Using a modular approach we showed that the depletion of cartilage ECM proteins is associated
331 with a decrease in glycolytic enzymes and a parallel activation of the adhesion mediated
332 cytoskeleton remodeling proteins (RhoA, RAC1) in chondrocytes obtained from late-stage
333 knee OA patients compared to healthy donors. Indentation-type atomic force microscopy in
334 biopsies from OA patients has revealed that the nano-stiffness of damaged cartilage is lower
335 than the healthy non-degraded cartilage and that OA cartilage becomes softer due to
336 progressive disintegration of the collagen meshwork³⁸. The observed depletion of ECM
337 proteins and the concurrent upregulation of CD44, a sensor of ECM integrity, indicate a shift
338 towards a low ECM adhesion microenvironment in OA³⁹. In low ECM adhesion conditions,
339 integrin signaling is dampened and integrin-anchored actin filaments become shorter and
340 fragmented⁴⁰. We found that key structural components of integrin activation and cytoskeleton
341 remodeling such as, TLN, vinculin (VCL), the Rho family GTPases RhoA and Rac1 as well as
342 structural components of the F-actin stress fibers and focal adhesions, actinin- α isoform 1
343 (ACTN1,) cluster in the center of the core chondrocyte network (Fig. 2, A). ACTN1 is abundant
344 in healthy chondrocytes and depleted in OA-derived ones, whereas F-actin depolymerizing
345 destrin (DSTN) is abundant in OA chondrocytes (Fig.2, A), indicating increased actin
346 remodeling in OA. Although the integrin activator and linker to actin filaments TLN is more
347 abundant in OA, VCL which stabilizes the interaction between TLN and the actin cytoskeleton
348 under high tension conditions, is depleted in OA chondrocytes. These interactions indicate an
349 adaptation of the ECM-focal adhesion interface to low ECM forces.

350 It has been shown that glycolytic pathway components are among the most upregulated
351 proteins during the early stages of chondrogenesis in OA and healthy hBMSCs, highlighting
352 the central role of glycolysis in chondrogenic differentiation²⁸. We found significant overlap
353 between the 43 altered proteins with the majority of the proteins mapping to MEyellow, which
354 is enriched for glycolysis/glucose metabolism proteins but also comprises key structural
355 components of the cartilage ECM as COL2A1, COL6A1, COL6A2 and actin polymerization
356 ACTN1, ACTN4) (Fig. 2A). Proteins mediating glycolysis and contributing to the formation

357 of cartilage ECM were found to be more abundant in healthy chondrocytes compared to OA,
358 suggesting that the link between ECM-cytoskeleton and glucose metabolism might play a role
359 in OA associated chondrocyte biology. Mechanosensing regulates glycolysis through
360 cytoskeletal remodeling by actomyosin stress fiber disassembly⁴⁰. Our findings are in line with
361 a recently described mechanism, where soft ECM causes stress fiber disassembly and release
362 of E3-ubiquitin ligase TRIM21, which targets phosphofructokinase (PFK) for degradation by
363 the proteasome thus reducing glycolysis. Although our data cannot provide direct functional
364 evidence for TRIM21-mediated PFK degradation, the concurrent depletion of structural ECM
365 components and the decrease in glycolytic mediators indicate a connection between
366 mechanosensing and glycolysis regulation in chondrocytes. Moreover, they suggest that
367 perturbations in ECM proteins in OA cartilage could modulate glucose metabolism in
368 chondrocytes.

369 Our analysis also showed that glucose-6-phosphate dehydrogenase (G6PD),-the first and rate
370 limiting enzyme in the pentose phosphate pathway (PPP) that catalyzes the conversion of
371 glucose-6-phosphate to ribose-5'-phosphate, is over abundant in OA compared to healthy
372 chondrocytes. In line with our findings, OA hBMSCs have increased levels of ribose-5'-
373 phosphate compared to healthy hBMCs on the 2nd day post chondrogenesis induction (d2pc)
374 indicating increased PPP flux²⁸. Importantly, ribose-5'-phosphate was higher in the core of the
375 OA hBMSC on day2pc micromass cultures. These results parallel the observations made in
376 MCF-10A cells grown in 3D cultures where glucose uptake decreases in centrally located cells
377 (ECM deprived/cell-cell adhesion stimulated). Furthermore, it has been demonstrated that
378 reduced glycolytic flux increases ROS, which is reduced by PPP derived NADH that rescues
379 ATP production and cell survival⁴¹. Importantly, the connection between low glycolytic flux
380 and ROS production is corroborated by the *in vivo* inhibition of glycolysis with monosodium
381 iodoacetate which induced ROS, auto-inflammation and enhanced OA progression in rats⁴³.
382 Taken together, our observations indicate that OA chondrocytes deprived of cell-ECM contacts
383 rely on adaptive metabolic switches, such as the PPP NADH-driven antioxidant rescue, the
384 alternative ATP production from FAO and alternative sources of acetyl-CoA import to the
385 TCA to survive the low-glycolytic flux. The adaptive antioxidant responses might explain why
386 superoxide dismutase levels are not increased in OA chondrocytes in response to excessive
387 ROS production which is a hallmark of OA and why BNTA induction of SOD3 increases ECM
388 biosynthesis and reduces inflammation in a mouse model⁴³⁻⁴⁵.

389 In addition, chondrocyte lipid peroxidation and not ROS has been shown to induce cartilage
390 matrix protein oxidation and degradation in OA but a connection with mechanosensing was

391 not established⁴⁶. We found that GPX4 was only detected in the OA interactome suggesting
392 that lipid peroxide scavenging activity is increased in OA. Recent studies in cancer cells
393 brought forward new insights into the role of cell-cell contacts in enhancing escape from
394 ferroptosis. In low cell density conditions, long-chain and highly unsaturated neutral TAGs
395 become enriched while de novo lipogenesis and desaturation pathways decrease leading to
396 increased PUFA uptake predisposing cells to ferroptosis⁴⁷.

397 Exclusive detection of APOE, C3, CRP and SERPINA1 only in healthy chondrocytes indicates
398 that in healthy individuals the detrimental effects of chronic inflammation might be attenuated
399 by an inflammation check-point mechanism mediated by an APOE-C1q complex similarly to
400 atherosclerosis and Alzheimer's disease²⁹. Both atherosclerosis and OA are a chronic
401 inflammatory diseases and oxidized-LDL has detrimental effects in their progression⁴⁸ and
402 CCC activation is elevated in OA compared to healthy synovial fluid and membranes⁴⁹.

403 Lack of strong or significant correlation between other modules and OA might be attributable
404 to the dichotomous trait analysis (OA vs healthy) and the small sample size. We observed that
405 changes in the level of protein abundance across the samples showed patterns indicative of
406 donor subgroups (data not shown). Our sample size however does not allow testing for
407 proteome-module based patient stratification. We anticipate that increasing the sample size and
408 obtaining information on additional comorbidities will yield associations between modules and
409 patient subgroups.

410

411 In conclusion, our unbiased systems proteomics approach recapitulates hallmarks of OA and
412 provides new insights into the connection between cartilage ECM sensing and adaptive
413 metabolic changes underlying OA. Further functional investigation of the dynamic crosstalk
414 between the mechanical ECM property changes and the chondrocyte cellular state will increase
415 our understanding of the molecular bridge underlying the adaptive cartilage changes that lead
416 to OA. Importantly, it will expedite the elucidation of the cellular-microenvironment and
417 systemic context where GWAS SNPs exert their effect as well as potential drug discovery.

418

419 **Acknowledgements**

420 A.D. and E.M. are supported by iStemTheOS, Grant No. MIS 5033630/ELKE5876 from the
421 "HFRI - Hellenic Foundation for Research & Innovation" available to A.T.

422

423 **Author Contributions**

424 A.D. and A.T. designed the study. A.D. analyzed the spectral imaging count data matrix,
425 prepared the figures and interpreted the results. A.E and K.C.T performed the original
426 proteomics analysis and produced the spectral count matrix. A.T., A.E., K.C.T., I.P., E.M. and
427 C.B. interpreted the results. A.D. wrote the first draft of the paper. All authors read and edited
428 the paper. A.T finalized the paper and provided funding for the study.

429

430 **Role of the funding source**

431 The funding source has no role in the study design, collection, analysis and interpretation of
432 data, nor in the writing of the manuscript and the decision to submit the manuscript for
433 publication.

434

435 **Conflict of Interest**

436 The authors declare no conflicts of interest.

437

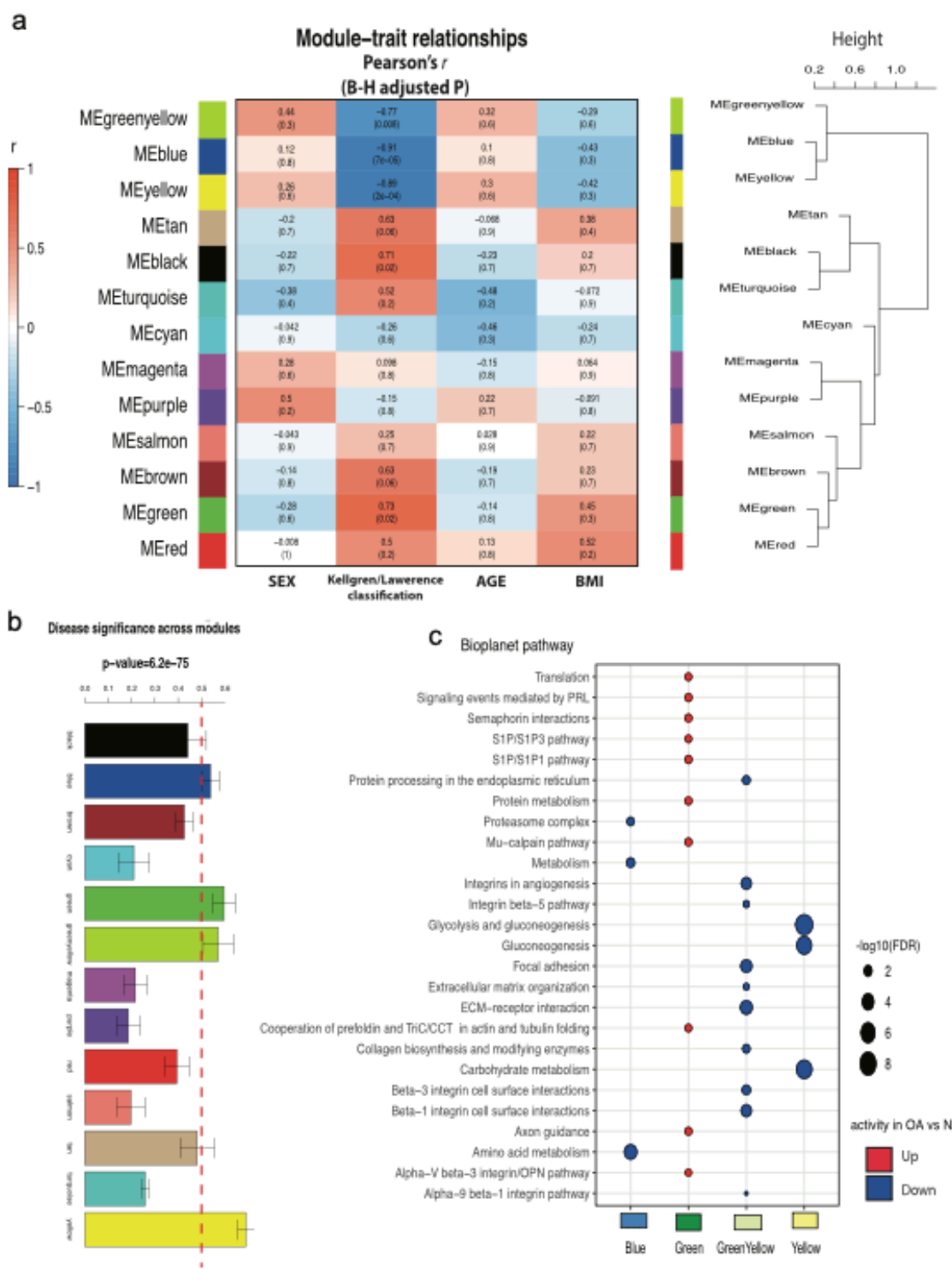
438 **References**

439

- 440 1. Cui, A., Li, H., Wang, D., Zhong, J., Chen, Y. & Lu, H. Global, regional prevalence,
441 incidence and risk factors of knee osteoarthritis in population-based studies.
442 *EClinicalMedicine* **29**(2020).
- 443 2. Tonge, D.P., Pearson, M.J. & Jones, S.W. The hallmarks of osteoarthritis and the
444 potential to develop personalised disease-modifying pharmacological therapeutics.
445 *Osteoarthritis Cartilage* **22**, 609-21 (2014).
- 446 3. Butterfield, N.C., Curry, K.F., Steinberg, J., Dewhurst, H., Komla-Ebri, D., Mannan, N.S.
447 *et al.* Accelerating functional gene discovery in osteoarthritis. *Nat Commun* **12**, 467
448 (2021).
- 449 4. Steinberg, J., Brooks, R.A., Southam, L., Bhatnagar, S., Roumeliotis, T.I., Hatzikotoulas,
450 K. *et al.* Widespread epigenomic, transcriptomic and proteomic differences between
451 hip osteophytic and articular chondrocytes in osteoarthritis. *Rheumatology (Oxford)*
452 **57**, 1481-1489 (2018).
- 453 5. Steinberg, J., Ritchie, G.R.S., Roumeliotis, T.I., Jayasuriya, R.L., Clark, M.J., Brooks, R.A.
454 *et al.* Integrative epigenomics, transcriptomics and proteomics of patient
455 chondrocytes reveal genes and pathways involved in osteoarthritis. *Sci Rep* **7**, 8935
456 (2017).
- 457 6. Steinberg, J., Southam, L., Butterfield, N.C., Roumeliotis, T.I., Fontalis, A., Clark, M.J. *et*
458 *al.* Decoding the genomic basis of osteoarthritis. *BioRxiv*
459 <https://doi.org/10.1101/835850>(2021).
- 460 7. Hartwell, L.H., Hopfield, J.J., Leibler, S. & Murray, A.W. From molecular to modular cell
461 biology. *Nature* **402**, C47-52 (1999).
- 462 8. Horvath, S., Zhang, B., Carlson, M., Lu, K.V., Zhu, S., Felciano, R.M. *et al.* Analysis of
463 oncogenic signaling networks in glioblastoma identifies ASPM as a molecular target.
464 *Proc Natl Acad Sci U S A* **103**, 17402-7 (2006).
- 465 9. Seyfried, N.T., Dammer, E.B., Swarup, V., Nandakumar, D., Duong, D.M., Yin, L. *et al.*
466 A Multi-network Approach Identifies Protein-Specific Co-expression in Asymptomatic
467 and Symptomatic Alzheimer's Disease. *Cell Syst* **4**, 60-72 e4 (2017).
- 468 10. Tsois, K.C., Bei, E.S., Papatheanasiou, I., Kostopoulou, F., Gkretsi, V., Kalantzaki, K. *et*
469 *al.* Comparative proteomic analysis of hypertrophic chondrocytes in osteoarthritis.
470 *Clin Proteomics* **12**, 12 (2015).
- 471 11. Romani, P., Valcarcel-Jimenez, L., Frezza, C. & Dupont, S. Crosstalk between
472 mechanotransduction and metabolism. *Nat Rev Mol Cell Biol* **22**, 22-38 (2021).
- 473 12. Zheng, L., Zhang, Z., Sheng, P. & Mobasheri, A. The role of metabolism in chondrocyte
474 dysfunction and the progression of osteoarthritis. *Ageing Res Rev* **66**, 101249 (2021).
- 475 13. Salinas, D., Mumey, B.M. & June, R.K. Physiological dynamic compression regulates
476 central energy metabolism in primary human chondrocytes. *Biomech Model*
477 *Mechanobiol* **18**, 69-77 (2019).
- 478 14. Karpievitch, Y.V., Dabney, A.R. & Smith, R.D. Normalization and missing value
479 imputation for label-free LC-MS analysis. *BMC Bioinformatics* **13 Suppl 16**, S5 (2012).
- 480 15. Zhang, Z. Multiple imputation with multivariate imputation by chained equation
481 (MICE) package. *Ann Transl Med* **4**, 30 (2016).
- 482 16. Risso, D., Ngai, J., Speed, T.P. & Dudoit, S. Normalization of RNA-seq data using factor
483 analysis of control genes or samples. *Nat Biotechnol* **32**, 896-902 (2014).

- 484 17. Langfelder, P. & Horvath, S. WGCNA: an R package for weighted correlation network
485 analysis. *BMC Bioinformatics* **9**, 559 (2008).
- 486 18. Huang, R., Grishagin, I., Wang, Y., Zhao, T., Greene, J., Obenauer, J.C. *et al.* The NCATS
487 BioPlanet - An Integrated Platform for Exploring the Universe of Cellular Signaling
488 Pathways for Toxicology, Systems Biology, and Chemical Genomics. *Front Pharmacol*
489 **10**, 445 (2019).
- 490 19. Kuleshov, M.V., Jones, M.R., Rouillard, A.D., Fernandez, N.F., Duan, Q., Wang, Z. *et al.*
491 Enrichr: a comprehensive gene set enrichment analysis web server 2016 update.
492 *Nucleic Acids Res* **44**, W90-7 (2016).
- 493 20. Szklarczyk, D., Gable, A.L., Lyon, D., Junge, A., Wyder, S., Huerta-Cepas, J. *et al.* STRING
494 v11: protein-protein association networks with increased coverage, supporting
495 functional discovery in genome-wide experimental datasets. *Nucleic Acids Res* **47**,
496 D607-D613 (2019).
- 497 21. Wickham, H. ggplot2: Elegant Graphics for Data Analysis. *Springer-Verlag New York*
498 (2016).
- 499 22. Barabasi, A.L., Gulbahce, N. & Loscalzo, J. Network medicine: a network-based
500 approach to human disease. *Nat Rev Genet* **12**, 56-68 (2011).
- 501 23. Ni, Z., Zhou, S., Li, S., Kuang, L., Chen, H., Luo, X. *et al.* Exosomes: roles and therapeutic
502 potential in osteoarthritis. *Bone Res* **8**, 25 (2020).
- 503 24. Jia, H., Ma, X., Tong, W., Doyran, B., Sun, Z., Wang, L. *et al.* EGFR signaling is critical for
504 maintaining the superficial layer of articular cartilage and preventing osteoarthritis
505 initiation. *Proc Natl Acad Sci U S A* **113**, 14360-14365 (2016).
- 506 25. Jeong, H., Mason, S.P., Barabasi, A.L. & Oltvai, Z.N. Lethality and centrality in protein
507 networks. *Nature* **411**, 41-2 (2001).
- 508 26. Goh, K.I., Cusick, M.E., Valle, D., Childs, B., Vidal, M. & Barabasi, A.L. The human
509 disease network. *Proc Natl Acad Sci U S A* **104**, 8685-90 (2007).
- 510 27. Sato, C., Iwasaki, T., Kitano, S., Tsunemi, S. & Sano, H. Sphingosine 1-phosphate
511 receptor activation enhances BMP-2-induced osteoblast differentiation. *Biochem*
512 *Biophys Res Commun* **423**, 200-5 (2012).
- 513 28. Rocha, B., Cillero-Pastor, B., Eijkel, G., Calamia, V., Fernandez-Puente, P., Paine, M.R.L.
514 *et al.* Integrative Metabolic Pathway Analysis Reveals Novel Therapeutic Targets in
515 Osteoarthritis. *Mol Cell Proteomics* **19**, 574-588 (2020).
- 516 29. Yin, C., Ackermann, S., Ma, Z., Mohanta, S.K., Zhang, C., Li, Y. *et al.* ApoE attenuates
517 unresolvable inflammation by complex formation with activated C1q. *Nat Med* **25**,
518 496-506 (2019).
- 519 30. Boeuf, S., Steck, E., Pelttari, K., Hennig, T., Buneb, A., Benz, K. *et al.* Subtractive gene
520 expression profiling of articular cartilage and mesenchymal stem cells: serpins as
521 cartilage-relevant differentiation markers. *Osteoarthritis Cartilage* **16**, 48-60 (2008).
- 522 31. Milner, J.M., Elliott, S.F. & Cawston, T.E. Activation of procollagenases is a key control
523 point in cartilage collagen degradation: interaction of serine and metalloproteinase
524 pathways. *Arthritis Rheum* **44**, 2084-96 (2001).
- 525 32. Corr, M. Wnt-beta-catenin signaling in the pathogenesis of osteoarthritis. *Nat Clin*
526 *Pract Rheumatol* **4**, 550-6 (2008).
- 527 33. Wang, Y., Fan, X., Xing, L. & Tian, F. Wnt signaling: a promising target for osteoarthritis
528 therapy. *Cell Commun Signal* **17**, 97 (2019).
- 529 34. Dao, D.Y., Jonason, J.H., Zhang, Y., Hsu, W., Chen, D., Hilton, M.J. *et al.* Cartilage-
530 specific beta-catenin signaling regulates chondrocyte maturation, generation of

- 531 ossification centers, and perichondrial bone formation during skeletal development. *J*
532 *Bone Miner Res* **27**, 1680-94 (2012).
- 533 35. Yang, W.S., SriRamaratnam, R., Welsch, M.E., Shimada, K., Skouta, R., Viswanathan,
534 V.S. *et al.* Regulation of ferroptotic cancer cell death by GPX4. *Cell* **156**, 317-331
535 (2014).
- 536 36. E., P., F., H., J., D., M., P., Toerne., v., A.C., K. *et al.* Cell density-dependent ferroptosis
537 in breast cancer is induced by accumulation of polyunsaturated fatty acid-enriched
538 triacylglycerides. *BioRxiv* (2021).
- 539 37. Moessinger, C., Kuerschner, L., Spandl, J., Shevchenko, A. & Thiele, C. Human
540 lysophosphatidylcholine acyltransferases 1 and 2 are located in lipid droplets where
541 they catalyze the formation of phosphatidylcholine. *J Biol Chem* **286**, 21330-9 (2011).
- 542 38. Stolz, M., Gottardi, R., Raiteri, R., Miot, S., Martin, I., Imer, R. *et al.* Early detection of
543 aging cartilage and osteoarthritis in mice and patient samples using atomic force
544 microscopy. *Nat Nanotechnol* **4**, 186-92 (2009).
- 545 39. Knudson, W. & Loeser, R.F. CD44 and integrin matrix receptors participate in cartilage
546 homeostasis. *Cell Mol Life Sci* **59**, 36-44 (2002).
- 547 40. Park, J.S., Burckhardt, C.J., Lazcano, R., Solis, L.M., Isogai, T., Li, L. *et al.* Mechanical
548 regulation of glycolysis via cytoskeleton architecture. *Nature* **578**, 621-626 (2020).
- 549 41. Schafer, Z.T., Grassian, A.R., Song, L., Jiang, Z., Gerhart-Hines, Z., Irie, H.Y. *et al.*
550 Antioxidant and oncogene rescue of metabolic defects caused by loss of matrix
551 attachment. *Nature* **461**, 109-13 (2009).
- 552 42. Yang, C., Ko, B., Hensley, C.T., Jiang, L., Wasti, A.T., Kim, J. *et al.* Glutamine oxidation
553 maintains the TCA cycle and cell survival during impaired mitochondrial pyruvate
554 transport. *Mol Cell* **56**, 414-24 (2014).
- 555 43. Huang, T.C., Chang, W.T., Hu, Y.C., Hsieh, B.S., Cheng, H.L., Yen, J.H. *et al.* Zinc Protects
556 Articular Chondrocytes through Changes in Nrf2-Mediated Antioxidants, Cytokines
557 and Matrix Metalloproteinases. *Nutrients* **10**(2018).
- 558 44. Ruiz-Romero, C., Calamia, V., Mateos, J., Carreira, V., Martinez-Gomariz, M.,
559 Fernandez, M. *et al.* Mitochondrial dysregulation of osteoarthritic human articular
560 chondrocytes analyzed by proteomics: a decrease in mitochondrial superoxide
561 dismutase points to a redox imbalance. *Mol Cell Proteomics* **8**, 172-89 (2009).
- 562 45. Shi, Y., Hu, X., Cheng, J., Zhang, X., Zhao, F., Shi, W. *et al.* A small molecule promotes
563 cartilage extracellular matrix generation and inhibits osteoarthritis development. *Nat*
564 *Commun* **10**, 1914 (2019).
- 565 46. Tikunov, M.L., Shah, R. & Allison, G.T. Evidence linking chondrocyte lipid peroxidation to
566 cartilage matrix protein degradation. Possible role in cartilage aging and the
567 pathogenesis of osteoarthritis. *J Biol Chem* **275**, 20069-76 (2000).
- 568 47. Lee, S.W., Rho, J.H., Lee, S.Y., Chung, W.T., Oh, Y.J., Kim, J.H. *et al.* Dietary fat-
569 associated osteoarthritic chondrocytes gain resistance to lipotoxicity through
570 PKCK2/STAMP2/FSP27. *Bone Res* **6**, 20 (2018).
- 571 48. Gkretsi, V., Simopoulou, T. & Tsezou, A. Lipid metabolism and osteoarthritis: lessons
572 from atherosclerosis. *Prog Lipid Res* **50**, 133-40 (2011).
- 573 49. Wang, Q., Rozelle, A.L., Lepus, C.M., Scanzello, C.R., Song, J.J., Larsen, D.M. *et al.*
574 Identification of a central role for complement in osteoarthritis. *Nat Med* **17**, 1674-9
575 (2011).
- 576
- 577



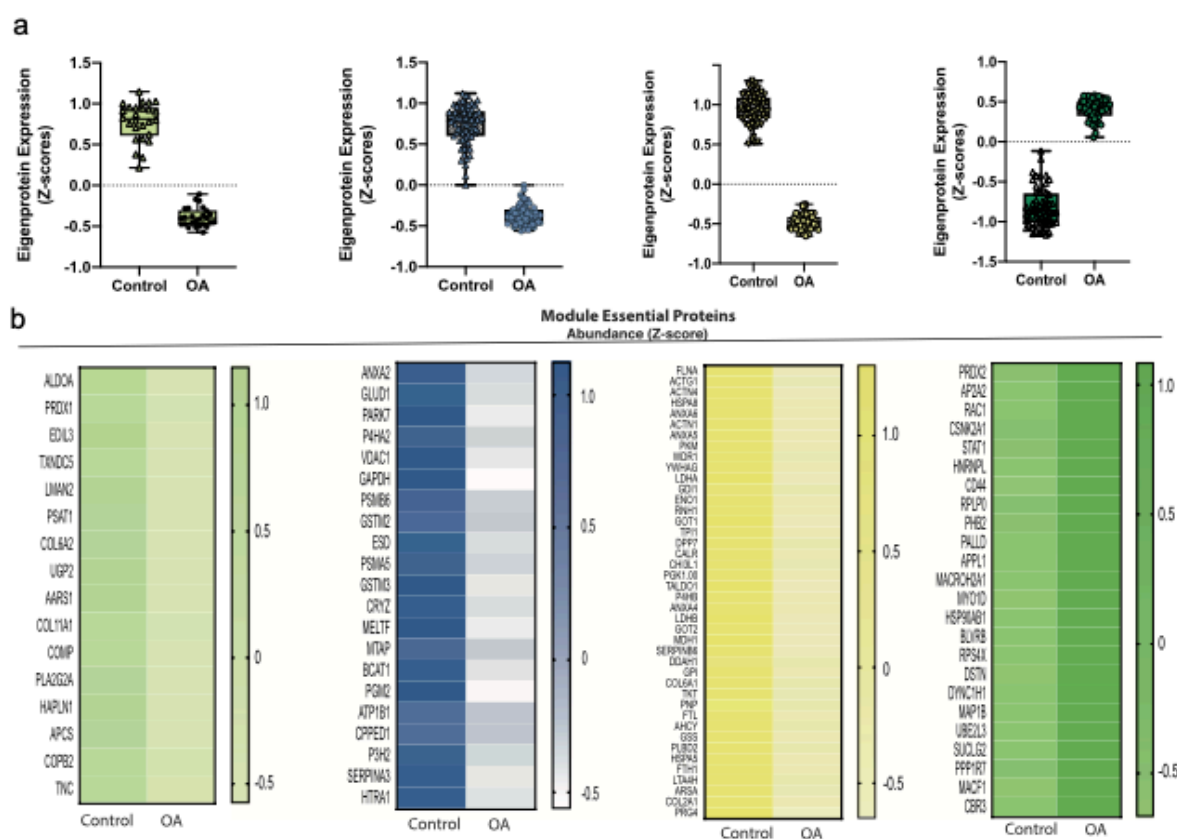
579

580 **Figure 1. Modular structure of the shared OA and healthy chondrocyte proteome**
581 **network**

582 **A.** The heatmap illustrates trait – module protein associations represented by Pearson
583 correlations and B-H adjusted P values. The dendrogram represents the hierarchical clustering
584 of the module protein levels across the samples **B.** Histograms show the mean of the correlation

585 coefficient for the module proteins as a measure of the association between protein levels and
 586 osteoarthritis (OA) termed disease significance (DS). The red dashed line marks $r=0.5$. C. The
 587 top enriched terms for the modules with $DS>0.5$. Red: over abundant in OA vs healthy, Blue:
 588 depleted in OA vs healthy D. Scaled abundance (Z-scores) of the module essential proteins.

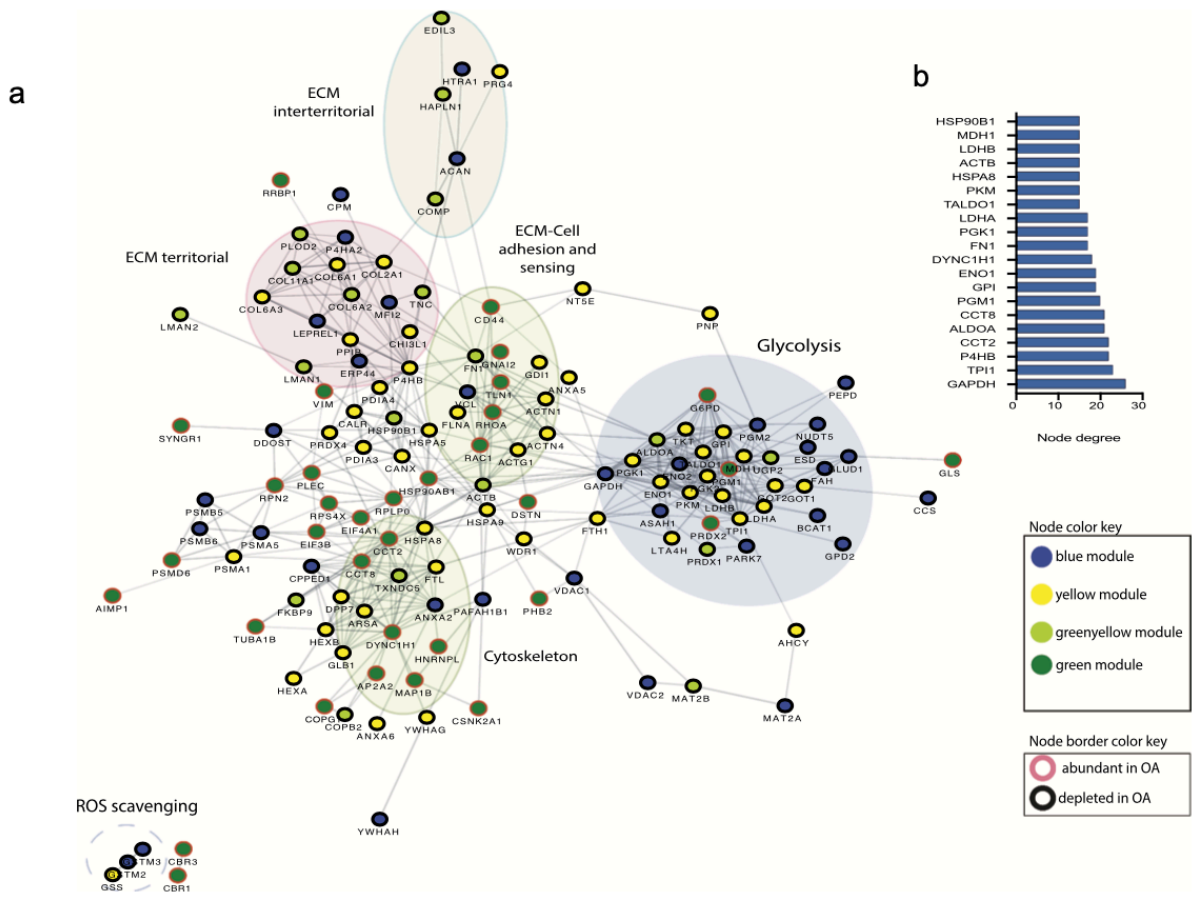
589
 590
 591
 592
 593



594
 595
 596
 597
 598
 599
 600
 601
 602
 603

Figure 2. Protein-protein interaction network on the module-eigen proteins representing the core chondrocyte interactome

A. Spring weighted layout applied to PPIs obtained from STRING database ($score>0.7$, high confidence). The nodes represent module proteins and the color represents their module membership. Node border color represents abundance levels in OA vs healthy chondrocytes, red: abundant in OA vs healthy, black: depleted in OA vs healthy. Edges represent STRING scores. The colored areas represent distinct functional clusters. **B.** Distribution of the number of edges (degree) for the top 20 nodes.

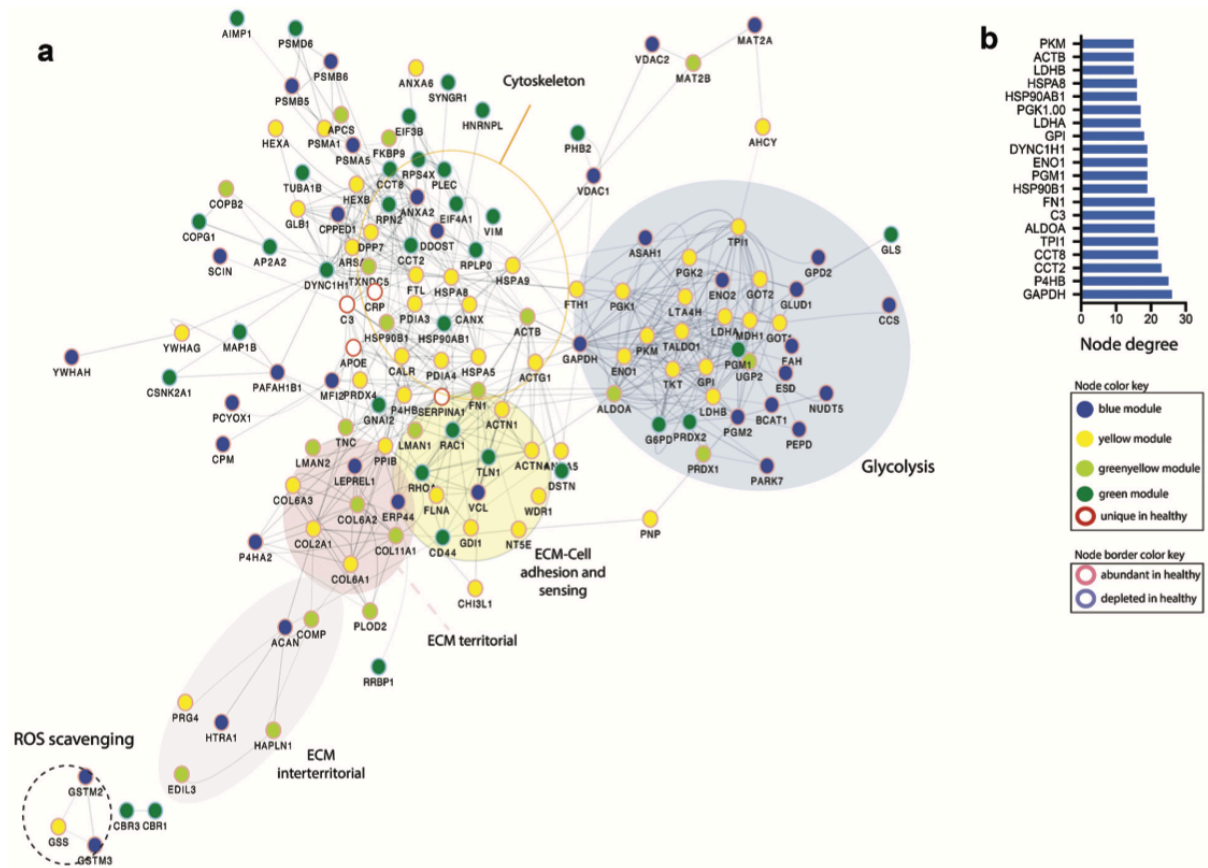


604

605 **Figure 3. Integrated protein-protein interaction networks mapping core chondrocyte and**
 606 **healthy interactomes**

607 **A.** Spring weighted layout applied to PPIs obtained from STRING database (score>0.7, high
 608 confidence). Nodes are proteins and edges represent STRING scores. The colored areas
 609 represent distinct functional clusters. **B.** Distribution of the number of edges (degree) for the
 610 top 20 nodes.

611

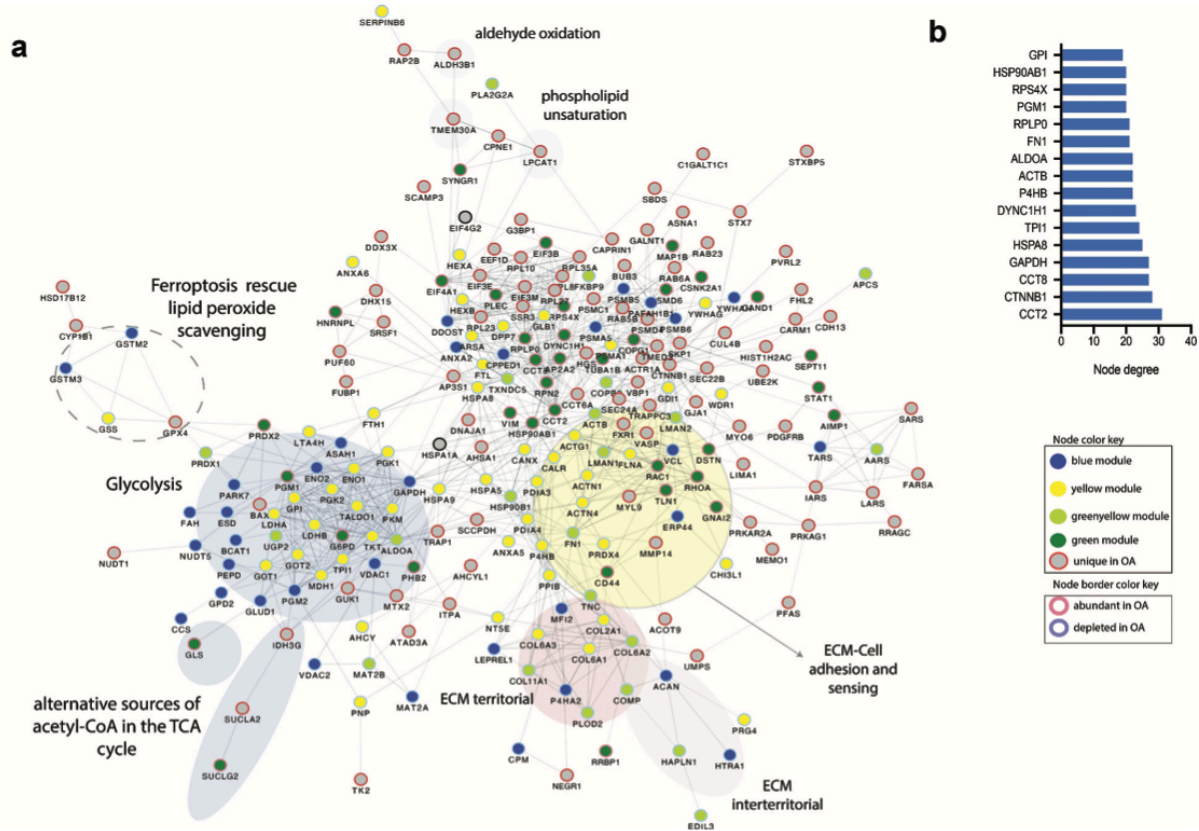


612

613 **Figure 4. Integrated protein-protein interaction networks mapping core**
 614 **chondrocyte and healthy interactomes.**

615 A. Spring weighted layout applied to PPIs obtained from STRING database (score>0.7, high
 616 confidence). Nodes are proteins and edges represent STRING scores. The colored areas
 617 represent distinct functional clusters. B. Distribution of the number of edges (degree) for
 618 the top 20 nodes.

619



620

621 **Figure 5. Integrated protein-protein interaction networks mapping core chondrocyte and**
 622 **OA interactomes**

623 **A.** Spring weighted layout applied to PPIs obtained from STRING database (score>0.7, high
 624 confidence). Nodes are proteins and edges represent STRING scores. The colored areas
 625 represent distinct functional clusters. **B.** Distribution of the number of edges (degree) for the
 626 top 20 nodes.